J Mol Model (2009) 15:1067–1078
DOI 10.1007/s00894-009-0456-7

ORIGINAL PAPER

Theoretical study of the geometrical and electronic structures and thermochemistry of spherophanes

Amar Saal · Claude August Daul · Thibaut Jarrosson · Ourida Ouamerali

Received: 4 November 2008 / Accepted: 18 December 2008 / Published online: 17 February 2009

Abstract A set of supramolecular cage-structures—spherophanes—was studied at the density functional B3LYP level. Full geometrical structure optimisations were made with 6–31G and 6–31G(d) basis sets followed by frequency calculations, and electronic energies were evaluated at B3LYP/6–31++G(d,p). Three different symmetries were considered: C1, Ci, and Oh. It was found that the bonds between the benzene rings are very long to allow π-electron delocalisation between them. These spherophanes show portal openings of 2.596 Å in Spher1, 4.000 Å in Meth2, 3.659 Å in Oxa3, and 4.412 Å in Thia4. From the point of view of potential host–guest interaction studies, it should also be noted that the atoms nearest to the centre of the cavities are carbons bonded to X groups. These supramolecules seem to exhibit relatively large gap HOMO−LUMO: 2.89 eV(Spher1), 5.26 eV(Meth2), 5.73 eV(Oxa3), and 4.82 eV(Thia4). The calculated $\Delta H°_f$ (298.15 K) values at B3LYP/6–31G(d) are (in kcal mol^{-1}) 750.98, 229.78, −10.97, and 482.49 for Spher1, Meth2, Oxa3, and Thia4, respectively. Using homodesmotic reactions, relative to Spher1, the spherophanes Meth2, Oxa3, and Thia4 are less strained by −399.13 kcal mol^{-1}, −390.40 kcal mol^{-1}, and −411.38 kcal mol^{-1}, respectively. Their infrared and ^{13}C NMR calculated spectra are reported.

Keywords Supramolecules · Spherophanes · Molecular cages · Thermochemistry · B3LYP · Strain energy

Electronic supplementary material The online version of this article (doi:10.1007/s00894-009-0456-7) contains supplementary material, which is available to authorized users.

A. Saal · C. A. Daul
Department of Chemistry, University of Fribourg,
Fribourg, Switzerland

T. Jarrosson
Ecole ENSCM,
Montpellier, France

A. Saal · O. Ouamerali (✉)
LPCTCI Laboratory, Faculty of Chemistry,
USTHB University of Algiers,
Algiers, Algeria
e-mail: oouamerali@hotmail.com

Introduction

Great interest is currently being devoted to the design and synthesis of new molecular cage materials, since these may be used to encapsulate molecules, radicals, ions, and atoms inside their cavities. This encapsulation feature is very useful for chemical applications as well as for industry. This technique has been widely used for isolating very unstable species, for example, by Warmuth et al. [1, 2] to isolate cyclohepta-1,2,4,6-tertaene and *o*-benzyne inside carcerands, and by Cram et al. [3] to isolate cyclobutadiene, also inside carcerands. Dolgonos et al. have demonstrated theoretically that the normally unstable smallest fullerene C_{20} acquires a certain stability when it is inserted inside large fullerenes [4] or inside the nearly spherical cavity of the tetraureacalix[4]arene dimer self-assembled molecular capsule [5].

Separation of reactive compounds by their encapsulation inside cavities has also been achieved. This approach has allowed spectroscopic studies and characterisation of reaction intermediates [6–8]. For example, the rearrangement of singlet phenylnitrene to 1-azacyclohepta-1,2,4,6-tetraene inside hemicarcerand has been achieved by Warmuth et al. [6].

The building blocks that are widely used for the preparation of molecular cages include (among others):

calixarenes [9, 10], resorcinarenes [11, 12], glycorils [13, 14], and spherands [15]. In order to facilitate the formation of the cage and avoid side compounds, preorganisation of the subunits is necessary and the use of template compounds is usually recommended [13, 14, 16, 17].

A fundamental difference between the many supramolecular cages that now exist is the bonding type assuring cohesion of the cage. These bonds determine the chemical, physical and chemical-physics properties of the cage. Covalent bonding leads to very stable supramolecules that are capable of permanently encapsulating guest molecules [18]. Non-covalent bond types such as hydrogen bonds, charge transfer interactions, van der Waals interactions, and metal coordination are weak and much less strong than covalent bonds. Thus, the relative stability of capsules made of these types of interactions is due only to the cooperative effects of the many existing interactions [19, 20]. Generally, these latter types of molecular capsules allow reversible capture of guests.

In this study, we consider a set of molecular containers. Formally, these molecules may be obtained by replacing each summit of a cube by a benzene ring. Spherophane1 (Spher1; molecular structure $C_{48}H_{24}$) is the simplest spherical molecule obtained by such a manipulation. Spher1 may be derived by adding 24 hydrogen atoms to the C_{48} fullerene studied by Dunlop and Taylor [21] or the designed structure 24(4,6,8) with 12 squares, eight hexagons and six octagons in the reference [22].

The electronic and geometrical structures of this spherophane were investigated at different model chemistries. In addition to Spher1, three other spherophanes, in which the edges of the cube are replaced by a linker, were considered (Fig. 1): a $–CH_2–$ group, yielding methanospherophane2 (Meth2); an –O– group, giving oxaspherophane3 (Oxa3); and an –S– group yielding thiaspherophane4 (Thia4). The molecular formulae of Meth2, Oxa3 and Thia4 are $C_{60}H_{48}$, $C_{48}H_{24}O_{12}$, and $C_{48}H_{24}S_{12}$, respectively [23, 24]. Such a

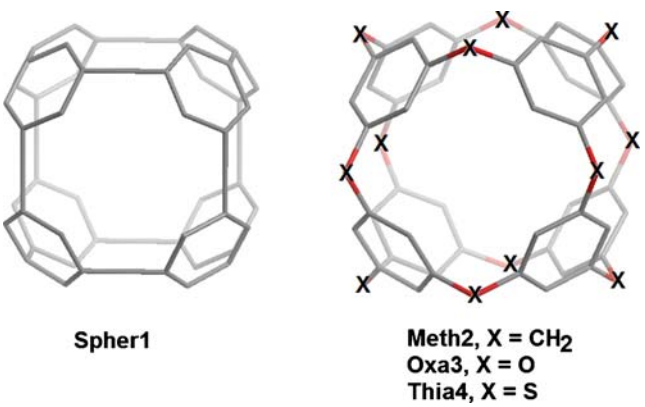

Fig. 1 Structures of the spherophanes considered in this study: *Spher1* Spherophane 1, *Meth2* Methanospherophane 2, *Oxa3* Oxaspherophane 3, and *Thia4* Thiaspherophane 4

manoeuvre enhances the volume of the inner cavity of Spher1 while decreasing its strained energy. This study will help to highlight these features.

All four spherophanes were studied theoretically with the aid of a quantum chemical ab initio method. Their geometrical parameters, electronic energies, and molecular orbital levels as well as their normal mode frequencies and thermochemistries were evaluated using different model chemistries.

Computational methods

Given the fixed purposes of this present study and the size of the molecules under consideration—more than 48 heavy atoms—we have used the following computational procedures.

First, complete optimisations of the geometrical parameters were performed using the well known density functional theory (DFT) combination Becke's three parameters hybrid functional (B3) with the Lee, Yang, and Parr (LYP) expression of non-local correlation (B3LYP) [25–27], with the Pople split-valence basis sets 6–31G and 6–31G(d) [28]. The B3LYP method has proven its accuracy in determining geometrical parameters [29, 30], electronic energies and thermochemical properties [31–34], and is used widely for studying structures and the stability of large molecules, fullerenes, and supramolecules [22, 29, 35, 36]. The basis sets 6–31G and 6–31G(d) have also been recommended for purposes such as the present study. From their study of 184 molecules, Scott and Radom [32] pointed out that B3LYP/6–31G(d) is a successful procedure in the prediction of harmonic fundamental vibrational frequencies. This level has also been recommended by Kassaee et al. [30] for the evaluation of entropies, and by Ventura et al. [37] for thermochemistry calculations.

B3LYP, which includes electron correlation effects, is ideally suited to the evaluation of thermochemical property values [31, 37]. Since determination of these parameters is also one of our objectives, frequency calculations were performed at both levels: B3LYP/6–31G and B3LYP/6–31G(d). Although relatively sophisticated computational resources were available. some frequency calculations took up to 10 days.

In order to eliminate systematic errors due to ab initio calculations, harmonic vibrational frequency scaling factors were used. These scaling factors depend only on the method and the basis set used. Because they are determined by comparing experimental and theoretical results of a set of molecules, slightly different values of such factors are found in the literature [30, 32, 38, 39]. Frequency calculations confirm the minimum states of the optimised geometries, and compute zero point energies, thermal

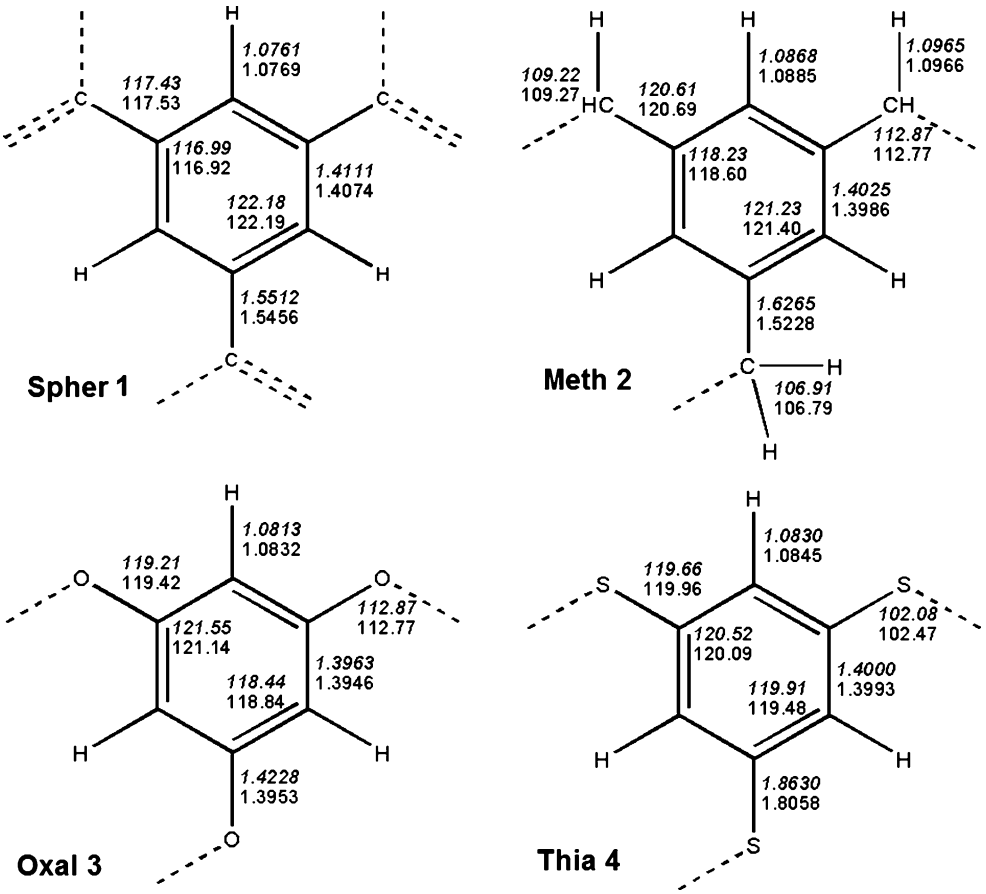

Fig. 2 Geometrical parameters of the spherophanes at octahedral symmetry obtained at B3LYP/6–31G (*upper values in italics*) and at B3LYP/6–31G(d) (*lower values*). Bond lengths are in Ångstroms and angles in degrees

corrections to internal energy, enthalpies, Gibbs free energies, and entropies as well as the constant heat capacities of these spherophanes. Scaling factors taken from the literature were also used to correct these properties.

To improve the accuracy of the calculated electronic energies, single point calculations were performed using the same method with the large basis set 6–31++G(d,p), which is 6–31G augmented with diffuse and polarised functions on all atoms.

All calculations were performed using the set of programs G03 [40]. For spatial representations and viewing of vibrations and orbitals, GaussView and Molden [41] were used.

Results and discussion

Geometrical structures

Complete geometrical structure optimisations were made at B3LYP level with the basis sets 6–31G and 6–31G(d). The molecules were placed in the symmetries Oh, Ci, and C1 during these calculations. For each spherophane type, the different symmetries seemed to exhibit almost the same values of bond lengths and angles. The values for geometrical parameters obtained at both levels of calculation of the octahedral molecules are given in Fig. 2.

From this figure, the results of bond lengths C–C, C–O, and C–S values obtained with the 6–31G(d) basis set are a

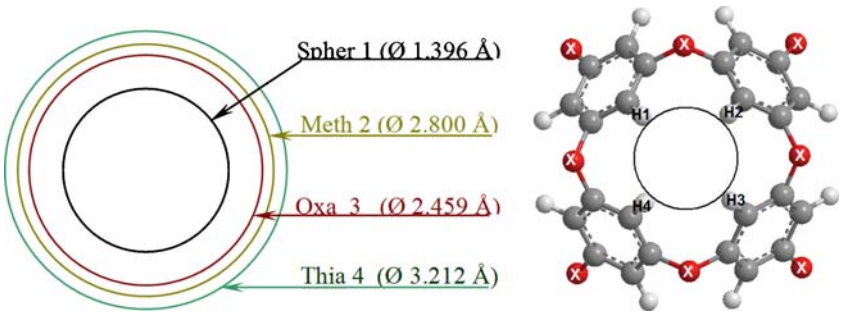

Fig. 3 Diameter at the entrance of the pores in the four spherophanes studied, evaluated at B3LYP/6–31G(d)

Table 1 $d_{H1,H2}$ and $d_{H1,H3}$ distances (Å) obtained at the B3LYP level. Atom designations are shown in Fig. 3. *Spher1* Spherophane 1, *Meth2* Methanospherophane 2, *Oxa3* Oxaspherophane 3, and *Thia4* Thiaspherophane 4

		Spher1	Meth2	Oxa3	Thia4
6–31G	H1...H2	1.8397	2.8347	2.6460	3.1916
	H1...H3	2.6017	4.0089	3.7420	4.5136
6–31G(d)	H1...H2	1.8359	2.8282	2.5873	3.1197
	H1...H3	2.5963	3.9997	3.6590	4.4119

bit less than those obtained with 6–31G, while Ph–H bonds are underestimated by the latter basis set. Furthermore, C–S and C–O bond lengths are more influenced by the introduction of the polarisation functions, although the C–O (or C–S) bond diminishes from 1.4228 Å (1.8630 Å) obtained with 6–31G to 1.3953 Å (1.8058 Å) obtained with 6–31G(d) basis set. However, the polarisation functions have hardly any affect on valence angles.

Figure 2 shows also that the nature of the linker between the phenyl rings affects the geometrical regularity of the benzenes. The valence angles show that the benzenes are more regular in the case of Thia4, while they are more distorted in the Spher1 molecule. The bond lengths between the benzene rings show that there is almost no π-electrons delocalisation out of the rings. Moreover, in the case of Spher1, these values seem to be a bit higher than the regular C–C simple bond length value, reflecting the fact that this spherophane is very strained.

It is also interesting to know the dimension of the pores. Thus, in Fig. 3 and Table 1, we report the distances between hydrogen atoms at the entrance of the holes. Distances $d_{H1,H2}$ and $d_{H1,H3}$ in the case of Thia4 and Oxa3, respectively, are more influenced by the polarisation function. The results show that $d_{H1,H2}$ and $d_{H1,H3}$ increase with the radius of the linker: Spher1λτ;λτ;Oxa3<Meth2<Thia4. In Fig. 3, we have drawn circles at the entrance of the spherophanes—the diameters correspond to $d_{H1,H3}$. Interactions between these hydrogen atoms are stronger in Spher1 than in the other three molecules. This perturbs the rest of the molecule and deforms the benzene ring structure.

Let us consider, for simplicity, the designation C_α, C_β, H_γ, and X_δ and their corresponding symmetric atoms C'_α, C'_β, C'_γ, and C'_δ with respect to their respective molecular centres. The distance between each atomic pair is shown in Table 2. The reported results show that the linker atoms (X) are further from the molecular centre than all the other atoms, while the designated $C\alpha$ carbon atoms are closest. In the case of Thia4, the C_α and C_β atoms are almost the same distance from the centre of the molecule. Thus, for subsequent guest insertion studies, these atoms must be considered first.

Electronic energies

Electronic energies, highest occupied molecular orbital (HOMO) and lowest unoccupied molecular orbital (LUMO) as well as the energy gaps $E_{LUMOHOMO}$ obtained with the four model chemistries B3LYP/6–31G//B3LYP/6–31G, B3LYP/6–31G(d)//B3LYP/6–31G(d), B3LYP/6–31++G(d,p)//B3LYP/6–31G, and B3LYP/6–31++G(d,p)//B3LYP/6–31G(d) are reported in Tables 2 and 3. Again, almost the same electronic energy values were found within the different symmetries. Such very small differences (less than 0.5 kcal mol^{-1}) are not sufficient to make any decision about the symmetry of the fundamental ground state.

Analysis of the results in Table 3 indicates that polarisation functions affect very strongly the values of the total electronic energies of the spherophanes. The difference between the electronic energies obtained with the basis sets 6–31 and 6–31G(d) is 270 kcal mol^{-1}, 339 kcal mol^{-1}, 489 kcal mol^{-1}, and 489 kcal mol^{-1} in the case of Spher1, Meth2, Oxa3, and Thia4, respectively. Furthermore, the value of the electronic energy diminishes in the order 6–31G//6–31G, 6–31G(d)//6–31G(d), 6–31++G(d,p)//6–31G, and then 6–31++G(d,p)//6–31G(d). This fact demonstrates that a single point calculation improves the accuracy of the energy.

The kinetic stability of a system is measured by the energies of the HOMO, LUMO, and by the gap $E_{LUMOHOMO}$. Table 4 lists the energies of the HOMO and LUMO obtained at B3LYP/6–31++G(d,p)//6–31G(d), and the $E_{LUMOHOMO}$ energy gaps of the studied spherophanes. The values obtained vary slightly with the model chemistry used. Moreover, the single point calculations affected the gaps by decreasing gap values obtained at the optimised level. This effect becomes more appreciable when the basis set used for optimisation is small. From the model B3LYP/6–31G//6–

Table 2 Distances (Å) between atoms obtained at B3LYP/6–31G(d). C'_α, C'_β, C'_γ, and C'_δ are the corresponding symmetric atoms of C_α, C_β, C_γ, and C_δ, respectively, relative to the molecular centre

Distances		Spher1	Meth2	Oxa3	Thia4
C_α	C_α'	7.280	8.837	0.437	9.270
C_β	C_β'	7.426	8.833	8.473	9.282
H_γ	H_γ'	8.268	9.754	9.416	10.204
X_δ	X_δ'	/	10.152	9.633	11.090

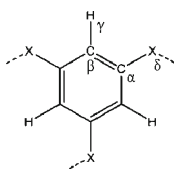

Table 3 Electronic energies of the spherophanes obtained at B3LYP with different basis sets (given in Hartree)

Molecule	Symmetry	6–31G// 6–31G	6–31++G(d,p)// 6–31G	6–31G(d)// 6–31G(d)	6–31++G(d,p)// 6–31G(d)
Spher1	Oh	−1,842.63903	−1,843.16097	−1,843.06919	−1,843.161424
	Ci	−1,842.63837	−1,843.16036	−1,843.06854	−1,843.160819
	C1	−1,842.63835	−1,843.16035	−1,843.06856	−1,843.160882
Meth2	Oh	−2,314.85500	−2,315.52479	−2,315.39309	−2,315.525067
	Ci	−2,314.85492	−2,315.52531	−2,315.39299	−2,315.525628
	C1	−2,314.85488	−2,315.52539	−2,315.39298	−2,315.525602
Oxa3	Oh	−2,745.27780	−2,746.16568	−2,746.06488	−2,746.178066
	Ci	−2,745.27811	−2,746.16604	−2,746.06497	−2,746.178586
	C1	−2,745.27794	−2,746.16611	−2,746.06501	−2,746.178671
Thia4	Oh	−6,621.01469	−6,621.87247	−6,621.80055	−6,621.897708
	Ci	−6,621.01419	−6,621.87292	−6,621.80009	−6,621.898161
	C1	−6,621.01409	−6,621.87312	−6,621.80015	−6,621.89846
	Th	−6,621.01469	−6,621.87247	IF[a]	IF[a]

[a] One imaginary frequency was found at B3LYP/6–31G(d)

31G to B3LYP/6–31++G(d,p)//6–31G [respectively, from B3LYP/6–31G(d)//6–31G(d) to B3LYP/6–31++G(d,p)//6–31G(d)] the $E_{LUMOHOMO}$ gap decreases at least by 0.21 eV (respectively by 010 eV), 0.32 eV (0.21 eV), 0.18 eV (0.17 eV), and by 0.35 eV (0.19 eV) for Spher1, Meth2, Oxa3, and Thia4, respectively.

These gap energies depend strongly upon the nature of the linker between the benzene rings. At the B3LYP/6–31++G(d,p)//6–31G(d) level, these gaps are, in increasing order: 2.89 eV (no linker), 4.82 eV(X = S), 5.26 eV(X = CH_2), and 5.73 eV(X = O). Compared to the gaps obtained in the case of fullerenes, these spherophanes seem to exhibit large LUMO−HOMO gaps. Shao et al. [42]. have reported this property for thousands of isomers of some 27 fullerene types; the highest gap values obtained at PBE1PBE/6–311G*//DFTB are 2.88 eV for C_{60}, 2.86 eV for C_{70}, and 2.64 eV for C_{72}. Some authors consider that the ionisation potential of a molecule is the value of the HOMO's energy taken with sign '+'. Following this consideration, the ionisation potentials of Spher1, Meth2, Oxa3, and Thia4 are 5.71 eV, 6.21 eV, 7.39 eV, and 6.89 eV, respectively.

Figure 4 shows the energetic diagrams of the octahedral spherophanes obtained at B3LYP/6–31++G(d,p)//6–31G(d)

Table 4 Highest occupied molecular orbital (HOMO) and lowest unoccupied molecular orbital (LUMO) orbital energies obtained at B3LYP/6–31++G(d,p) of the different molecules studied as well as the gaps ($E_{LUMOHOMO}$) evaluated with different basis sets. Results were obtained at the correlated B3LYP and are given in electron volts

Molecule	Symmetry	6–31++G(d,p)//6–31G(d) HOMO	6–31++G(d,p)//6–31G(d) LUMO	Gap (eV) 6–31G//6–31G	6–31++G(d,p)//6–31G	6–31G(d)//6–31G(d)	6–31++G(d,p)//6–31G(d)
Spher1	Oh	−5.71	−2.82	3.10	2.89	2.99	2.89
	Ci	−5.71	−2.82	3.10	2.89	2.99	2.89
	C1	−5.71	−2.82	3.11	2.90	3.00	2.89
Meth2	Oh	−6.21	−0.94	5.57	5.25	5.47	5.26
	Ci	−6.21	−0.94	5.57	5.25	5.47	5.26
	C1	−6.21	−0.94	5.58	5.25	5.47	5.26
Oxa3	Oh	−7.38	−1.65	5.95	5.77	5.90	5.73
	Ci	−7.39	−1.66	5.95	5.77	5.90	5.73
	C1	−7.39	−1.66	5.95	5.77	5.91	5.73
Thia4	Oh	−6.88	−2.06	5.31	4.96	5.01	4.82
	Ci	−6.89	−2.07	5.31	4.96	5.01	4.82
	C1	−6.89	−2.07	531	4.96	5.01	4.82
	Th	[a]	[a]	5.31	4.96	IF[a]	IF[a]

[a] One imaginary frequency has been found at B3LYP/6–31G(d)

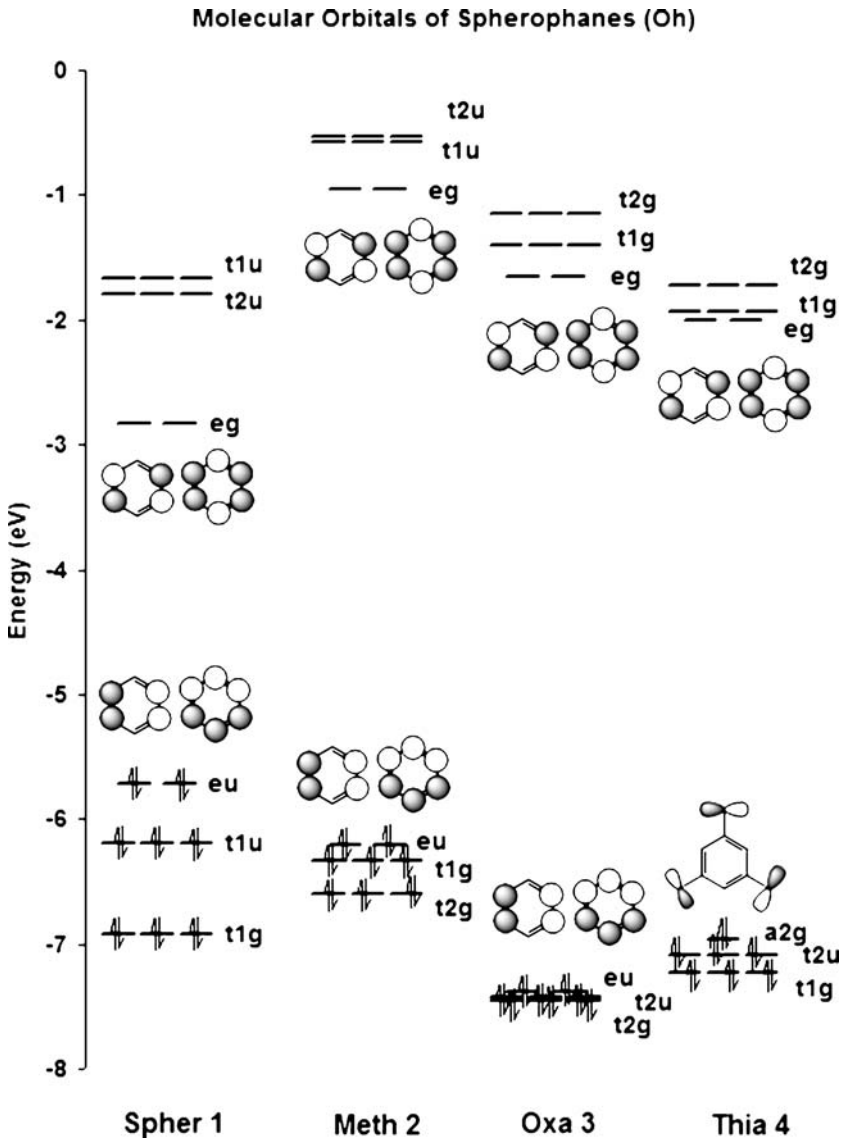

Fig. 4 Energetic diagram of the octahedral spherophanes. Only border orbitals are shown as well as a schematic form of the highest occupied molecular orbital (HOMO) and the lowest unoccupied molecular orbital (LUMO)

level by representing, for clarity, only the border levels: HOMO−2, HOMO−1, HOMO, LUMO, LUMO+1, and LUMO+2. The chemical reactivity of the studied systems is related to their HOMO and LUMO energies. This figure demonstrates, by considering the Fukui border orbitals principle, that, against nucleophile reactants, the reactivity of the spherophanes decreases in the order Spher1, Thia4, Oxa3, and then Meth2. However, against electrophiles their reactivity decreases in the order Spher1, Meth2, Thia4, and Oxa3.

By examining closely the shape of the HOMO and LUMO orbitals (Fig. 4), it was noted that, for Spher1 and Meth2, these doubly degenerated molecular orbitals correspond exactly to π-HOMO and π*-LUMO of a free benzene ring and their symmetries are e_u (HOMO) and e_g (LUMO). This is in agreement with what was previously deduced from the bond lengths study: each benzene ring keeps its own π-electrons. A very big difference was noted in the case of the Oxa3 molecule, where the HOMO corresponds to the π-HOMO of the benzenes; however, in the LUMO, the 4s and 4p orbitals of the oxygen atoms present a very small contribution, which could be neglected. In the case of Thia4, the LUMO of symmetry e_g corresponds to π*-LUMO of the benzenes; on the other hand, the HOMO is completely different. The HOMO of Thia4 has a symmetry of a_{2g} and essentially corresponds to a combination with the same coefficients of two 3p orbitals of each sulphur atom.

Table 5 Spin-orbital symmetry of the octahedral spherophanes

Molecule	Symmetry of the electronic spin orbitals
Spher1	$24e_u$, $42t_{1g}$, $72t_{1u}$, $72t_{2g}$, $48t_{2u}$, $28e_g$, $10a_{2u}$, $2a_{1u}$, $12a_{1g}$, $2a_{2g}$
Meth2	$28e_u$, $48t_{1g}$, $90t_{2g}$, $96t_{1u}$, $66t_{2u}$, $40e_g$, $12a_{2u}$, $4a_{2g}$, $18a_{1g}$, $2a_{1u}$
Oxa3	$28e_u$, $66t_{2u}$, $90t_{2g}$, $54t_{1g}$, $40e_g$, $96t_{1u}$, $4a_{2g}$, $16a_{1g}$, $12a_{2u}$, $2a_{1u}$
Thia4	$6a_{2g}$, $84t_{2u}$, $66t_{1g}$, $78e_g$, $114t_{1u}$, $32e_u$, $108t_{2g}$, $20a_{1g}$, $14a_{2u}$, $2a_{1u}$

The molecular nomenclatures of the octahedral spherophanes according to their orbital symmetries are given in Table 5.

Vibrational frequencies and spectroscopy

The fundamental normal modes vibrational frequencies of the four spherophanes were estimated at B3LYP with the basis 6–31G and 6–31G(d) and scaled by the factors 0.962 [39] and 0.9613 [40], respectively. Table S1 in the Supplementary material lists all the scaled fundamental vibrational frequencies values calculated at B3LYP/6–31G(d). Due to the high considered Oh symmetry, there is only a limited number of infrared and Raman active normal modes. Within this symmetry, only the t_{1u} modes are infra-red (IR) active and only t_{2g}, e_g, and a_{1g} modes are active in Raman. The scaled frequencies of these active modes for the different spherophanes are listed in Table 6.

IR intensities calculated at the B3LYP/6–31G(d) level are shown in Fig. 5. Figure 6 shows the ^{13}C NMR shift values obtained at B3LYP/6–31G(d), with tetramethylsilane (TMS) as a reference peak. Due to the high symmetry under consideration, the IR spectra are very simple. The ^{13}C NMR spectra show two and three types of carbon atoms. One can see that the high electronegativity of oxygen has affected the shifts of the carbons. However, in the case of Thia4, the peaks of the carbons are closer, which could be due to the long C–S distance and to the electronegativity values of the S and H atoms.

Thermochemistry and strain energy

The standard molar enthalpies of formation of the different spherophanes were calculated at all the levels considered. This property describes the thermodynamic stability of the compound at given conditions of pressure and temperature. Generally, two types of reactions are used to determinate the enthalpy of formation of a compound: isogyric reactions (spin conservation) and, most commonly, isodesmic reactions (bonds types conservation). Such reaction types lead to substantial cancellation of systematic errors due to the ab initio calculations, thus they give values close to the experimentally determined $\Delta_f H°$. For the present study, we considered the set of isodesmic reactions shown in Table 7. The experimental standard enthalpies of formation of the auxiliary simple molecules in these reactions are also given in this table. For molecules CH_4, C_6H_6, C_3H_8, CH_3–O–CH_3, and CH_3–S–CH_3, we performed DFT calculations with the same models as those used for the spherophanes in each case.

Table 6 Infra-red (IR) and Raman active normal modes scaled frequencies obtained at B3LYP/6–31G(d)

Molecule	Γ_i		Vibrational frequencies (cm^{-1})
Spher1	t_{1u}	IR active	293, 412, 586, 652, 712, 848, 916, 980, 1111,1169,1349, 1538, 3152, 3180
	t_{2g}	Raman active	138, 222, 415, 524, 645, 745, 813, 836, 961, 1074, 1142
	e_g	Raman active	182, 470, 511,869, 928,1169,1378, 1534, 3180
	a_{1g}	Raman active	362, 693, 895, 1002, 1198, 3180
Meth2	t_{1u}	IR active	172, 230, 322, 487, 543, 635, 731,857, 865, 891, 972, 979, 1152, 1253, 1296, 1438, 1457, 1590, 2933, 2973, 3047, 3050
	t_{2g}	Raman active	88, 159, 254, 468, 571, 657, 726, 840, 868, 930, 977, 1137, 1161, 1249, 1299, 1450, 1460, 1595, 2933, 3043, 3048
	e_g	Raman active	63, 258, 323, 461, 703, 853, 891, 954, 1152, 1439, 1458, 1597, 2933, 2973, 3050
	a_{1g}	Raman active	203,579, 735, 893, 980, 1258, 1457, 2934, 3051
Oxa3	t_{1u}	IR active	197, 258, 382, 481, 556, 633, 705, 831, 870, 982, 992, 1110, 1270, 1483, 1578, 3116, 3121
	t_{2g}	Raman active	109, 178, 277, 463, 593, 648, 707, 815, 854, 960, 983, 1096, 1276, 1432, 1588, 3112, 3116
	e_g	Raman active	67, 287, 379, 455, 711, 862, 930, 1094, 1431, 1594, 3121
	a_{1g}	Raman active	230, 531, 708, 875, 990, 1270, 3121
Thia4	t_{1u}	IR active	152, 191, 229, 371, 417, 537, 678, 765, 871, 901, 972, 1091, 1102, 1377, 1536, 3102, 3103
	t_{2g}	Raman active	72, 135, 228, 367, 412, 565, 670, 765, 863, 892, 969, 1085, 1102, 1382, 1539, 3100, 3102
	e_g	Raman active	44, 196, 262, 383, 596, 768, 905, 1103, 1380, 1541, 3103
	a_{1g}	Raman active	164, 393, 685, 881, 975, 1103, 3104

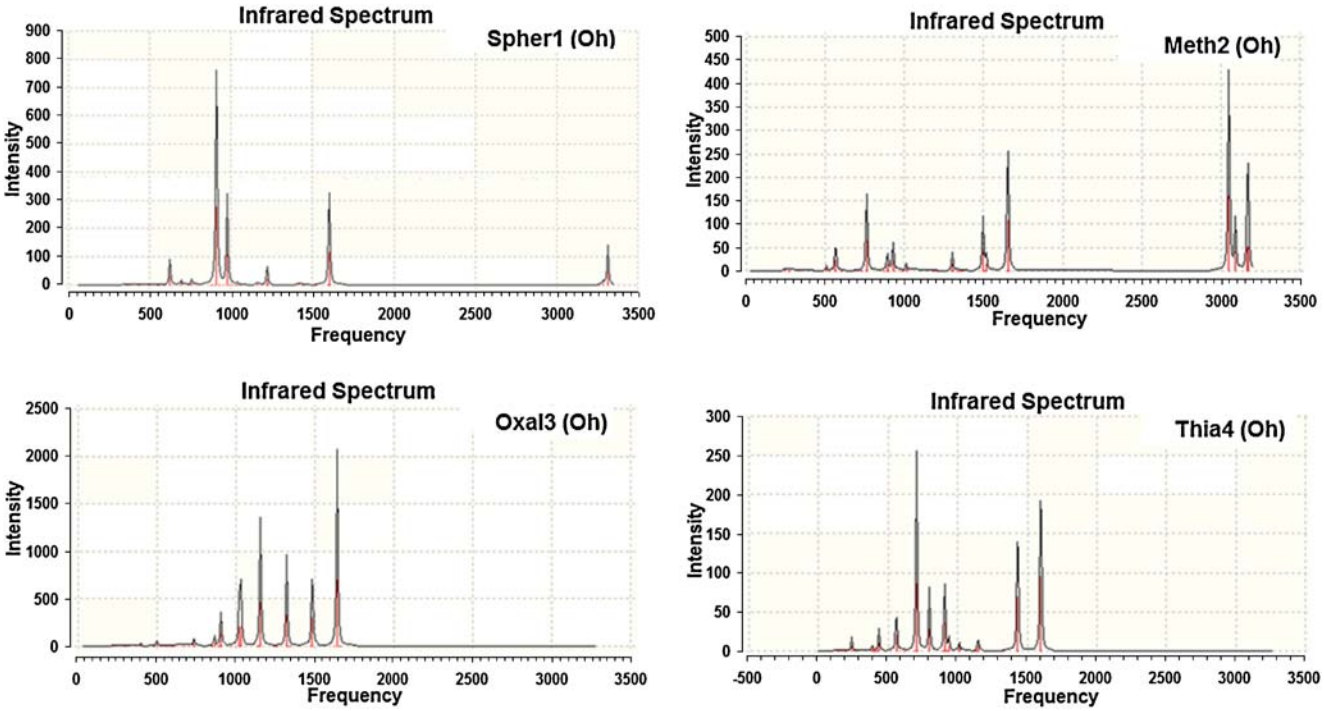

Fig. 5 Infra-red (IR) spectra of the octahedral spherophanes obtained at B3LYP/6–31G(d)

The calculated standard enthalpies of formation values at 298.15 K are given in Table 8. The formation of oxaspherophane is exothermic while the formation reactions of the other three spherophanes are endothermic. Δ_f H° of these spherophanes diminishes in the order Spher1>Thia4>Meth2>Oxa3.

In order to calibrate the results presented here, we propose to estimate—at the same level of calculation, i.e. B3LYP/6–31G(d)—the enthalpies of formation of a set of related structure molecules: biphenyl (PhPh), diphenylmethane ($PhCH_2Ph$), diphenyl ether (PhOPh), and diphenyl sulphide (PhSPh). Complete optimisations of these molecules and frequency calculations were performed. Using isodesmic reactions (Reactions 5–8 in Table 7) with similar auxiliary products, we determined the following enthalpies of formation (in kcal mol^{-1}): 43.43 (PhPh), 32.88 ($PhCH_2Ph$), 12.38 (PhOPh), and 55.23 (PhSPh), which are very close to the experimental values given in Table 7.

In the diphenyl derivatives there is no strain energy. Their optimised structures show that the angle C_{Ph}–X–C_{Ph} is equal to 114.76° in the case of $PhCH_2Ph$, 120.90° in PhOPh, and 103.66° in PhSPh, and the angle formed between the planes of the benzene rings is 40.08° in PhPh, 88.37° in $PhCH_2Ph$, 67.78° in PhOPh, and 69.80° in PhSPh.

The stability of the spherophanes and their diphenyl derivatives relative to free benzene rings is shown by means of the calculated enthalpies of reactions reported in Table 7; Reactions 9–12 show a negative ΔH of reaction, which means that dissociation of the spherophanes into their corresponding diphenyls is exothermic.

Now let us discuss the relative strain energy between the studied spherophanes. Consider first isodesmic Reaction (13) (Scheme 1).

The reaction enthalpy of (13), $\Delta H_r(13) = -7.78$ kcal mol^{-1}, is a measure of the enthalpy variation when the sulphur bridge between the phenyl rings is replaced by an ether bridge.

In Reaction (14) (Scheme 2), the bridges between the spherophanes and the diphenyls are interchanged. If the replacement of the ether bridges by sulphur bridges in the 12 diphenyl ether molecules involves the same variation in enthalpy as when this replacement occurs in Oxa3, and vice-versa, then $\Delta H_r(14)$ would be equal to zero. In that case, the difference between the enthalpies of formation of Thia4 and

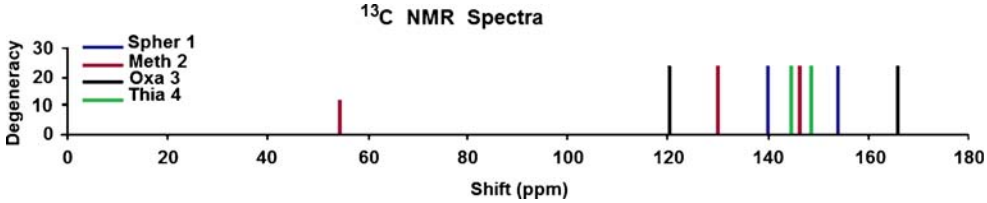

Fig. 6 ^{13}C NMR spectra of the octahedral spherophanes obtained at B3LYP/6–31G(d). Zero corresponds to the shift of tetramethylsilane (TMS) [HF/6–31G(d)]

Table 7 Isodesmic reactions used for calculation of standard molar enthalpies. Experimental standard enthalpies of formation ($\Delta_f H°$; 298.15 K) values of the auxiliary compounds used are also listed [43]

Reaction						Calculated molar enthalpy of reactions (kcal mol^{-1})
1	$C_{48}H_{24}$	+ 18 CH_4	⟶	8 C_6H_6	+ 6 C_3H_8	−421.23
2	$C_{60}H_{48}$	+ 24 CH_4	⟶	8 C_6H_6	+ 12 C_3H_8	56.42
3	$C_{48}H_{24}O_{12}$	+ 24 CH_4	⟶	8 C_6H_6	+ 12 CH_3OCH_3	69.44
4	$C_{48}H_{24}S_{12}$	+ 24 CH_4	⟶	8 C_6H_6	+ 12 CH_3SCH_3	−3.56
5	$C_{12}H_{10}$	+ (3/2) CH_4	⟶	2 C_6H_6	+ (1/2) C_3H_8	10.44
6	$C_{13}H_{12}$	+ 2 CH_4	⟶	2 C_6H_6	+ C_3H_8	17.40
7	$C_{12}H_{10}O$	+ 2 CH_4	⟶	2 C_6H_6	+ CH_3OCH_3	18.92
8	$C_{12}H_{10}S$	+ 2 CH_4	⟶	2 C_6H_6	+ CH_3SCH_3	11.06
9	$C_{48}H_{24}$	+ 12 CH_4	⟶	4 $C_{12}H_{10}$	+ 4 C_3H_8	−463.27
10	$C_{60}H_{48}$	+ 16 CH_4	⟶	4 $C_{13}H_{12}$	+ 8 C_3H_8	−11.78
11	$C_{48}H_{24}O_{12}$	+ 16 CH_4	⟶	4 $C_{12}H_{10}O$	+ 8 CH_3OCH_3	−6.03
12	$C_{48}H_{24}S_{12}$	+ 16 CH_4	⟶	4 $C_{12}H_{10}S$	+ 8 CH_3SCH_3	−47.69

Experimental standard enthalpies of formation

Compound	$\Delta_f H°_{298K}$(kcal mol^{-1})	Compound	$\Delta_f H°_{298K}$(kcal mol^{-1})
Biphenyl ($C_{12}H_{10}$)	43.36	CH_4	−17.83
Diphenylmethane ($C_{13}H_{12}$)	33.22	C_3H_8	−25.02
Diphenylether ($C_{12}H_{10}O$)	12.43	C_6H_6	19.82
Diphenylsulphide ($C_{12}H_{10}S$)	55.3	CH_3OCH_3	−44.00
		CH_3SCH_3	−8.96

Oxa3 is 12 times that between diphenyl sulphide and diphenyl ether, since

$$\Delta H_r(14) = \left[\Delta H_f(\text{Thia4}) - \Delta H_f(\text{Oxa3})\right] + 12 \times \left[\Delta H_f(\text{PhSPh}) - \Delta H_f(\text{PhOPh})\right].$$

However, the reaction enthalpy of (14) is found to be equal to −20.98 kcal mol^{-1}, and the difference $\left[\Delta H_f(\text{Thia4}) - \Delta H_f(\text{Oxa3})\right]$ is 11.51 times the difference $\left[\Delta H_f(\text{PhSPh}) - \Delta H_f(\text{PhOPh})\right]$. Reaction (14) may be considered as the sum of 12×Reaction (13) and Reaction (15) (Scheme 3), with $\Delta H_r(15)$ = 72.38 kcal mol^{-1}.

Reaction (15) is isodesmic and $\Delta H_r(15)$ is a measure of the dissociation/formation of the spherophane cages and of the dissociation/formation of the bridged diphenyls (PhSPh or PhOPh) to/from dimethylether or dimethylsulphide and benzene.

Reaction (14) is a homodesmotic reaction and its reaction enthalpy corresponds to the relative strain energy between Thia4 and Oxa3. $\Delta H_r(14)$ is negative, therefore Thia4 is less strained than Oxa3 by 20.98 kcal mol^{-1}.

Table 8 Standard molar enthalpies of formation at 298.15 K of the spherophanes obtained at B3LYP and different basis sets. The values are in kcal mol^{-1}

Molecule	Symmetry	6–31G// 6–31G	6–31++G(d,p)// 6–31G	6–31G(d)// 6–31G(d)	6–31++G(d,p)// 6–31G(d)
Spher1	Oh	594.65	598.02	750.59	602.50
	Ci	595.05	598.39	750.98	602.86
	C1	595.10	598.43	750.98	602.83
Meth2	Oh	129.27	140.99	229.78	145.92
	Ci	129.18	140.53	229.68	145.40
	C1	128.06	139.33	229.76	145.49
Oxa3	Oh	−110.72	−68.04	−10.97	−72.65
	Ci	−110.62	−67.97	−10.78	−72.73
	C1	−110.67	−68.18	−10.81	−72.80
Thia4	Oh	401.18	410.10	482.49	399.35
	Ci	401.27	409.60	482.54	398.83
	C1	401.38	409.52	482.49	398.63
	Th	401.18	410.10	IF[a]	IF[a]

[a] One imaginary frequency was found at B3LYP/6–31G(d)

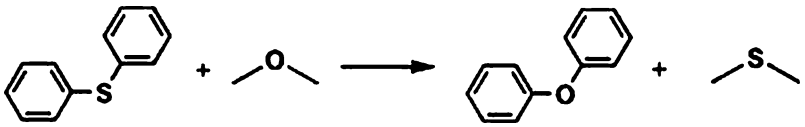

Scheme 1 Isodesmic reaction (13)

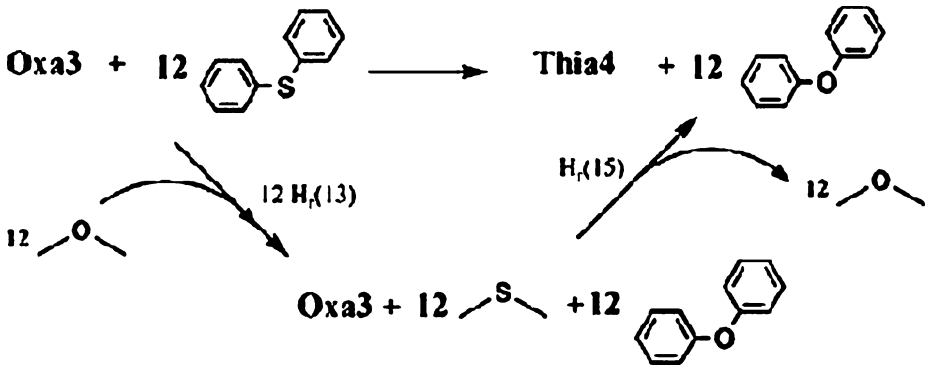

Scheme 2 Homodesmotic reaction (14)

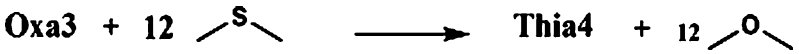

Scheme 3 Isodesmic reaction (15)

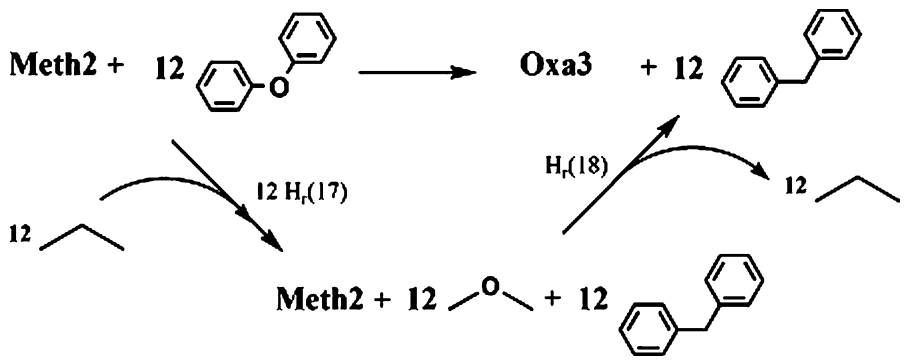

Scheme 4 Homodesmotic reaction (16)

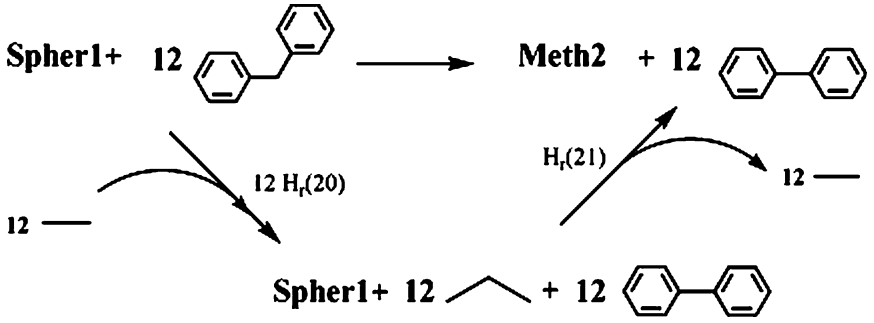

Scheme 5 Homodemotic reaction (19)

The relative strain energies between Meth2 and Oxa3 may be calculated via the homodesmotic Reaction (16) (Scheme 4).

Reaction (16) is endothermic, with a variation of enthalpy of 8.73 kcal mol^{-1}, thus Oxa3 is more strained than Meth2 by that quantity of energy. Finally, the homodesmotic Reaction (19) (Scheme 5) is very exothermic and Spher1 is highly strained than Meth2 by 399.13 kcal mol^{-1}.

To summarise, the least strained spherophane is Thia4, followed by Meth2, then Oxa3, and the most strained is Spher1.

Summary and outlook

The current study studied the electronic and geometrical structures of a set of novel cage-structure supramolecules—spherophanes—at the hybrid functional B3LYP level.

The results show that there is no π-electron conjugation between the phenyl rings, and that the nature of the linker between the benzene rings affects the geometrical parameters of the spherophanes. The geometrical structure of the benzenes is more distorted when the linker is a simple C–C bond and is more regular in the case of Thia4; this could be related to long-distance interactions between hydrogen atoms. Furthermore, the size of the inner cavity of these spherophanes increases in the order Spher1<Oxa3<Meth2<Thia4.

It was also found that, relative to C_{60} and C_{70} fullerenes, which exhibit high HOMO−LUMO gaps, the energy gaps of these spherophanes are higher. This gap increases in the order: Spher1<Thia4<Meth2<Oxa3. Apart from the HOMO of thiaspherophane, the border molecular orbitals HOMO and LUMO of these spherophanes have the same structures as those of benzene. However, the HOMO of Thia4 is constituted essentially by a combination with the same proportions of two 3p orbitals of the sulphur atoms.

The normal modes active in IR and Raman were also determined. ^{13}C NMR and IR spectra were also reported. Isodesmic reactions were used to evaluate standard molar enthalpies at 298.15 K. The results show that the formation of Oxa3 is exothermic. However, the strain structure of Spher1 is the more endothermic, its $\Delta_f H°(298.15\ K)$ is 595.24 kcal mol^{-1}. Using homodesmotic reactions, relative to Spher1, the

Table 9 Results of B3LYP/6–31G(d) calculations. U_{ther} (kcal mol^{-1}) Thermal energy, C_V (cal mol^{-1} Kelvin) heat capacity, S (cal mol^{-1} Kelvin) internal thermal correction to the energy

		6–31G(d)			6–31G(d) [a]		
Molecule	Symmetry	U_{ther}	C_v	S	U_{ther}	C_v	S
Spher1	Oh	364.10	136.84	161.40	361.06	127.18	145.40
	Ci	364.07	137.33	172.46	361.05	127.60	152.95
	C1	364.09	137.35	172.06	361.06	127.62	152.82
Meth2	Oh	586.60	193.63	229.87	525.99	65.04	95.22
	Ci	586.38	193.85	237.52	525.82	65.10	101.63
	C1	586.44	193.89	237.93	525.90	65.08	101.63
Oxa3	Oh	399.48	180.32	216.35	399.48	180.32	216.35
	Ci	399.73	180.06	222.58	399.73	180.06	222.58
	C1	399.72	180.08	222.59	399.72	180.08	222.59
Thia4	Oh	385.17	201.09	262.49	366.64	143.94	164.94
	Ci	384.92	201.31	272.38	366.40	144.12	171.51
	C1	384.90	201.37	272.27	366.38	144.17	171.55

[a] Corrected by the contribution of some of the low vibrational modes

spherophanes Meth2, Oxa3, and Thia4 are less strained by −399.13 kcal mol^{-1}, −390.40 kcal mol^{-1}, and −411.38 kcal mol^{-1}, respectively. For use in future experimental studies, Table 9 list the entropy, heat capacity, and internal thermal correction to the energy for each spherophane.

Further investigations, consisting of studying the capability of these spherophanes to store small molecules such as hydrogen, are in progress.

Acknowledgements A.S. thanks le Ministère Algérien de l'Enseignement Supérieur et de la Recherche Scientifique (MESRS) for financial support, and the Service Informatique of the University of Fribourg for providing computational facilities.

References

1. Warmuth R (1997) Angew Chem Int Ed Engl 36:1347
2. Warmuth R, Marvel MA (2000) Angew Chem Int Ed 39:1117
3. Cram DJ, Tanner ME, Thomas R (1991) Angew Chem Int Ed Engl 30:1024
4. Dolgonos G (2003) Fullerenes Nanotubes Carbon Nanostruct 11:155
5. Dolgonos G, Lukin O, Elstner M, Peslherbe GH, Leszczynski J (2006) J Phys Chem A 110:9405
6. Warmuth R, Macowiec S (2005) J Am Chem Soc 127:1085
7. Cram DJ, Tanner ME, Thomas R (1991) Angew Chem Int Ed Engl 30:1024
8. Makeiff DA, Vishnumurthy K, Sherman JC (2003) J Am Chem Soc 125:9558
9. Gutsche CD, Dhawan B, No KH, Muthukrishnan R (1981) J Am Chem Soc 103:3782
10. Gonzalez JJ, Ferdani R, Albertini E, Blasco JM, Arduini A, Pochini A, Prados P, de Mendoza J (2000) Chem Eur J 6:73
11. Högberg AGS (1980) J Am Chem Soc 102:6046
12. McGillivray LR, Atwood JL (1997) Nature 389:469
13. Branda N, Wyler R, Rebek J (1994) Science 263:1267
14. Rebek J (1999) Acc Chem Res 32:278
15. Cram DJ, Kaneda T, Helgeson RC, Lein GMJ (1979) Am Chem Soc 101:6752
16. Rebek J (2000) Chem Commun 8:637
17. Chapman RG, Sherman JC (1998) J Org Chem 63:4103
18. Gibb CLD, Stevens ED, Gibb BC (2000) Chem Commun 3:363
19. Gibb CLD, Stevens ED, Gibb BC (2001) J Am Chem Soc 123:5849
20. Fochi F, Jacopozzi P, Wegelius E, Rissanen K, Cozzini P, Marastoni E, Fisicaro E, Manini P, Fokkens R, Dalcanal E (2001) J Am Chem Soc 123:7539
21. Dunlap BI, Taylor R (1994) J Phys Chem 98:11018
22. Wu HS, Xu XH, Jiao H (2004) J Phys Chem 108:3813
23. Cram DJ (1983) Science 219:1177
24. Ross RS, Pincus P, Wudl F (1992) J Phys Chem 96:6169
25. Becke AD (1993) J Phys Chem 98:5648
26. Lee C, Yang W, Parr RG (1988) Phys Rev B 37:785
27. Miehlich B, Savin A, Stoll H, Preuss H (1989) Chem Phys Lett 157:200
28. Hariharan PC, Pople JA (1972) Chem Phys Lett 66:217
29. Sándor KM, Kornélia S, István B, Géza N, László K (2004) Tetrahedron Lett 45:1387
30. Kassaee MH, Keffer DJ, Steele WV (2007) J Mol Struc THEOCHEM 802:23
31. Ribeiro da Silva MAV, Matos MAR, Rio CA, Morais VMF, Wang J, Nichols G, Chickos JS (2000) J Phys Chem A 104:1774
32. Scott AP, Radom L (1996) J Phys Chem 100:16502
33. Sun H, Chen CJ, Bozzelli JW (2000) J Phys Chem A 104:8270
34. da Silvia G, Bozzelli JW (2007) J Phys Chem A 111:12026
35. Zhao X (2005) J Phys Chem B 109:5267
36. Shimotani H, Dragoe N, Kitazawa K (2001) J Phys Chem A 105:4980
37. Ventura ON, Kieninger M, Cachau RE (1999) J Phys Chem A 103:147
38. NIST Computational Chemistry Comparison and Benchmark Database, NIST Standard Reference Database Number 101. Release 14, Sept 2006, Editor: Johnson RD III http://srdata.nist.gov/cccbdb
39. Foresman JB, Frisch A (1996) Exploring chemistry with electronic structure methods, 2nd edn. Gaussian Inc, Wallingford, CT
40. Frisch MJ, Trucks GW, Schlegel HB, Scuseria GE, Robb MA, Cheeseman JR, Montgomery JA Jr, Vreven T, Kudin KN, Burant JC, Millam JM, Iyengar SS, Tomasi J, Barone V, Mennucci B, Cossi M, Scalmani G, Rega N, Petersson GA, Nakatsuji H, Hada M, Ehara M, Toyota K, Fukuda R, Hasegawa J, Ishida M, Nakajima T, Honda Y, Kitao O, Nakai H, Klene M, Li X, Knox JE, Hratchian HP, Cross JB, Adamo C, Jaramillo J, Gomperts R, Stratmann RE, Yazyev O, Austin AJ, Cammi R, Pomelli C, Ochterski JW, Ayala PY, Morokuma K, Voth GA, Salvador P, Dannenberg JJ, Zakrzewski VG, Dapprich S, Daniels AD, Strain MC, Farkas O, Malick DK, Rabuck AD, Raghavachari K, Foresman JB, Ortiz JV, Cui Q, Baboul AG, Clifford S, Cioslowski J, Stefanov BB, Liu G, Liashenko A, Piskorz P, Komaromi I, Martin RL, Fox DJ, Keith T, Al-Laham MA, Peng CY, Nanayakkara A, Challacombe M, Gill PMW, Johnson B, Chen W, Wong MW, Gonzalez C, Pople JA (2003) Gaussian 03, revision D.01. Gaussian Inc, Wallingford, CT
41. Schaftenaar G, Noordik JH (2000) Molden: a pre- and post-processing program for molecular and electronic structures. J Comput Aided Mol Des 14:123
42. Shao N, Gao Y, Zeng XC (2007) J Phys Chem C 111:17671
43. Lide DR (1992–1993) CRC handbook of chemistry and physics, 73rd edn. CRC, Boca Raton; www.openmopac.net/Downloads/PM6%20AM1%20PM3%20Main-Group%20raw%20data.xls